

# HARMONIZED SPECULATIVE SAMPLING

Lefan Zhang, Xiaodan Wang, Yanhua Huang\*, Ruiwen Xu

Xiaohongshu Inc.

Shanghai, China

{lefan, xiaodan2, yanhuahuang, ruiwenxu}@xiaohongshu.com

## ABSTRACT

Speculative sampling has proven to be an effective solution to accelerate decoding from large language models, where the acceptance rate significantly determines the performance. Most previous works on improving the acceptance rate focus on aligned training and efficient decoding, implicitly paying less attention to the linkage of training and decoding. In this work, we first investigate the linkage of training and decoding for speculative sampling and then propose a solution named HARMONIZED Speculative Sampling (HASS). HASS improves the acceptance rate without extra inference overhead by harmonizing training and decoding on their objectives and contexts. Experiments on three LLaMA models demonstrate that HASS achieves 2.81x-3.65x wall-clock time speedup ratio averaging across three datasets, which is 8%-15% faster than EAGLE-2.

## 1 INTRODUCTION

Generative large language models (LLMs), such as GPT-4 (Achiam et al., 2023) and LLaMA (Touvron et al., 2023), achieve impressive capabilities on various tasks. However, it is challenging to efficiently decode from LLMs because of the auto-regressive decoding mechanism, limiting their usage to time-sensitive applications. Speculative sampling (Chen et al., 2023a; Leviathan et al., 2023) addresses this by utilizing more concurrency from extra resources. In particular, it employs an efficient draft model to generate draft tokens auto-regressively and then verifies them by the target LLM in parallel. According to the verification result, a subset of draft tokens maintaining the same distribution of the target LLM is accepted as the decoding output.

Leviathan et al. (2023) shows that the higher acceptance rate leads to more wall-clock time acceleration and less extra computation resources. Most of previous works on improving the acceptance rate fall into two categories: aligned training (Li et al., 2024a; Zhou et al., 2023; Liu et al., 2023) and efficient decoding (Li et al., 2024b; Miao et al., 2024; Sun et al., 2024; Chen et al., 2023b). The former aims to obtain well-aligned draft models that behave similarly to the target LLM before the decoding stage, while the latter tries to gain more concurrency efficiently during the decoding stage. However, these works usually consider the training and decoding separately, paying less attention to the linkage between them on their objectives and contexts.

During the decoding stage, the objective of draft models is to propose tokens that the target LLM may give high probabilities (Li et al., 2024b; Miao et al., 2024; Sun et al., 2024). In this case, the draft model should spend more on the recall of desired tokens, and the order of these tokens can be appropriately weakened. On the other hand, most LLM applications perform nucleus sampling (Holtzman et al., 2019) or top-k sampling (Fan et al., 2018). For such decoding objectives, tokens with high probabilities have a more significant impact on the result. Consequently, with precious capacity to build efficient draft models, the training objective of draft models should be aware of above properties in the decoding stage. To the best of our knowledge, previous works on training draft models for speculative sampling are independent of these decoding properties.

To demonstrate the disharmony of training and decoding on contexts, we take EAGLE (Li et al., 2024a) as an example. EAGLE employs previous hidden states of the target LLM to generate subsequent draft tokens, which performs excellent acceptance rates with an efficient draft model. Note that other approaches utilizing hidden states of the target LLM, such as GLIDE (Du et al., 2024) and

\*Corresponding author.

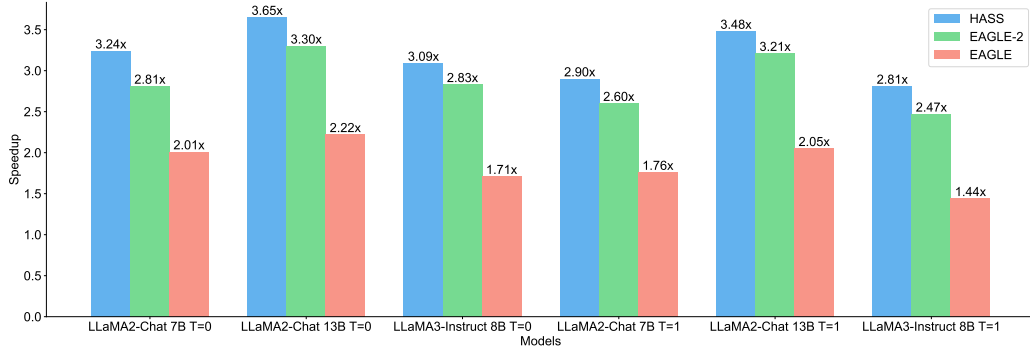


Figure 1: Speedup ratios of different methods on LLaMA2-Chat 7B/13B and LLaMA3-Instruct 8B with temperature  $T \in \{0, 1\}$ , averaging over MT-bench, HumanEval, and GSM8K datasets.

Clover (Xiao et al., 2024), are also suitable for the following analysis. As shown in Figure 2, the draft model always has access to the target LLM’s hidden states in previous timesteps during training. However, during the decoding stage, the draft model can not access the target LLM’s hidden states about unverified timesteps, leading to the context misalignment of training and decoding. One can view this issue as a kind of exposure bias (Bengio et al., 2015; Wang & Sennrich, 2020) at the feature level in speculative sampling.

In this paper, we thus propose a solution named HARMONIZED SPECULATIVE SAMPLING (HASS) that improves the acceptance rate by harmonizing training and decoding on their objectives and contexts. Specifically, to make draft models aware of the decoding strategy, HASS extends the idea about ranking distillation (Tang & Wang, 2018) from the recommender system to speculative sampling, resulting in a distillation loss concerning most probable tokens w.r.t. the target distribution. To harmonize training and decoding on their contexts, HASS employs a context-aligned training strategy to address the context misalignment discussed before. These two strategies of HASS improve the acceptance rate without any inference overhead and are also efficient during training.

We conduct experiments across dialogue, code generation, and mathematical reasoning using the MT-bench, HumanEval, and GSM8K datasets, respectively. LLaMA2-Chat 7/13B and LLaMA3-Instruct 8B are considered as target LLMs. Building with EAGLE-2 (Li et al., 2024b), HASS achieves 8%-12% acceptance length improvement over EAGLE-2, resulting in 2.81x-3.65x wall-clock time acceleration compared with the vanilla inference on a single NVIDIA H800 GPU.

## 2 PRELIMINARY

**Speculative sampling** is an implementation of speculative execution (Kung & Robinson, 1981; Hennessy & Patterson, 2011) for reducing wall-clock time by utilizing more concurrency. Specifically, given the target LLM  $\mathcal{M}^{(l)}$  intended for acceleration, speculative sampling employs a draft model  $\mathcal{M}^{(s)}$  to speculatively and efficiently generate draft tokens. The standard approach (Leviathan et al., 2023; Chen et al., 2023a) breaks down the next step generation into three steps:

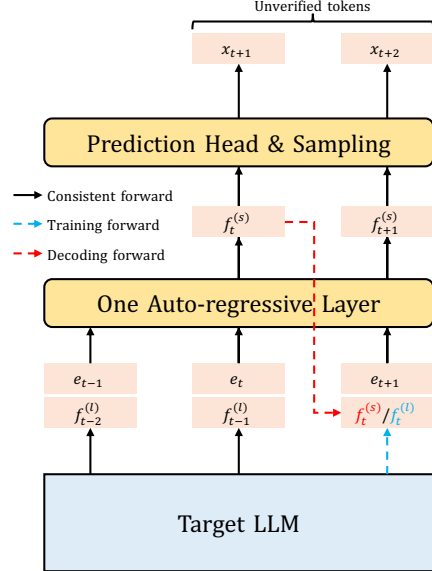


Figure 2: We use EAGLE (Li et al., 2024a) as an example to illustrate the context misalignment, where the speculation starts from timestep  $t$ .  $f^{(l)}$  and  $f^{(s)}$  represent hidden states from the target LLM and the draft model, respectively. When decoding draft token  $x_{t+2}$ , the input context is inconsistent between training and decoding.

- $\mathcal{M}^{(s)}$  proposes an unverified draft sequence with length  $L$  by auto-regressive decoding.
- $\mathcal{M}^{(l)}$  evaluates posterior probabilities of  $L$  draft tokens in parallel.
- $\tau$  tokens that maintain the target distribution are accepted by a modified rejection sampling schema based on the draft sequence and the distribution gap.

Leviathan et al. (2023) proves that the wall-clock time improvement ratio is proportional to  $\tau$  and the arithmetic operation increment ratio is inversely proportional to  $\tau$ . Consequently,  $\tau$ , known as the acceptance length, is vital for the acceleration performance. Similar analysis is also suitable when utilizing multiple draft sequences (Miao et al., 2024; Li et al., 2024b;a; Sun et al., 2024).

Note that  $\tau$  is highly related to the distribution gap between the target LLM and the draft model. With efficient decoding requirements, the draft model usually has limited capacity, leading to an unbridgeable distribution gap with the target LLM. Fortunately, during inference, the acceptance rate is mainly determined by the distribution alignment on desired tokens, i.e., tokens that the target LLM gives high probabilities. However, previous speculative sampling works mainly focus on the entire vocabulary set w.r.t. knowledge distillation from the target LLM (Li et al., 2024a; Zhou et al., 2023), which separates the training from the practical requirements of the decoding.

**EAGLE** (Li et al., 2024a) is a lightweight draft model design, as shown in Figure 2. During decoding, EAGLE utilizes the LM Head of the target LLM to generate draft tokens. Specifically, suppose that the speculation starts from timestep  $t$ , i.e., the first draft token is at timestep  $t + 1$ . When generating draft token  $x_{t+1}$ , target LLM’s hidden state  $f_{t-1}^{(l)}$  in second-to-top-layer is concatenated with the embedding  $e_t$  to perform the input of the draft model. During training, EAGLE constructs a regression task between  $f^{(l)}$ s and the draft model’s predicted hidden states  $f^{(s)}$ s.

However, because of the auto-regressive decoding, the draft model only accesses the target LLM’s features at the start of the speculation. EAGLE employs produced features of draft models as input in the following steps. This context misalignment caused by the feature inaccuracy introduces error accumulation and impairs the performance of generating later draft tokens. EAGLE-2 (Li et al., 2024b) employs the same model design but works on dynamic drafting structures instead of a static tree structure during the decoding stage, still leaving the above issue.

### 3 METHODOLOGY

As described in Sec. 2, previous speculative sampling methods focus on one of the training and decoding, ignoring the linkage on their objectives and contexts. In this section, we introduce HARMONIZED SPECULATIVE SAMPLING (HASS) to address the disharmony issues above. In particular, HASS consists of two parts: harmonized objective distillation and harmonized context alignment.

#### 3.1 HARMONIZED OBJECTIVE DISTILLATION

HASS pays more attention to desired tokens by leveraging the ranking distillation (Tang & Wang, 2018) idea from the recommender system. In particular, ranking distillation aims to learn a student model that gives higher ranks for the teacher model’s top ranking of items. In speculative sampling, the draft model and the target LLM act as the student and the teacher, respectively. Draft models with similar properties will perform at a higher acceptance rate in the decoding stage. Let the set of  $K$  tokens with the highest probabilities from the target LLM’s probability distribution as  $\hat{\Omega} \subset \Omega$ , where  $\Omega$  is the entire vocabulary. HASS considers the following Top- $K$  distillation loss:

$$L_{\text{Top-}K} = - \sum_{x \in \hat{\Omega}} q(x) \log p(x), \quad (1)$$

where  $q$  and  $p$  are the next token probability distributions of the target LLM and the draft model, respectively. The training objective above is designed to generate tokens that are friendly to the decoding strategies without extra computation overhead during inference. Note that, when building with EAGLE, the training stage can obtain  $\hat{\Omega}$  from hidden states of the target LLM, i.e., the proposed loss also enjoys the efficient training cost as EAGLE.

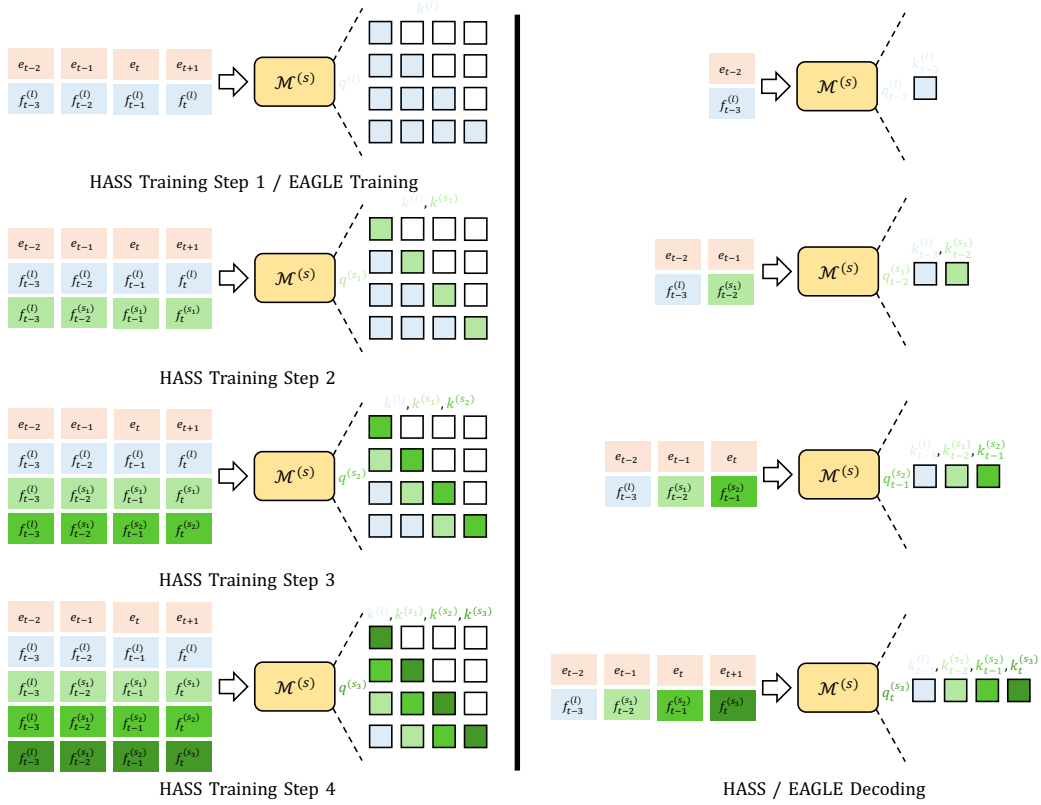


Figure 3: Training with harmonized context alignment, where  $q$  and  $k$  refer to the query and key states in the transformer layer, respectively. Superscript  $(l)$  denotes tensors from the target LLM, and superscript  $(s_j)$  denotes tensors from the  $j$ -th draft model forward. Note that during training  $(s_j)$  refers to call  $j$  times draft model in a batch, while during inference  $(s_j)$  refers to  $j$ -th autoregressive decoding.

### 3.2 HARMONIZED CONTEXT ALIGNMENT

HASS follows a context alignment schema that harmonizes training and decoding on their contexts. In particular, HASS divides the training procedure into  $n$  steps so that the draft model can access contextual features that are consistent with the decoding stage, as described below:

- The first step is the same as the training stage of EAGLE. Given timestep  $t + 1$ , the draft model takes the target model’s hidden feature  $f_t^{(l)}$  as input and produces the draft feature  $f_{t+1}^{(s_1)}$ . Here, the attention mask is the original causal mask without modification.
- The second step takes the first step’s features into account. For instance, in the self-attention mechanism of timestep  $t + 1$ ,  $f_t^{(s_1)}$  is used to calculate the current query, with keys and values from  $f_{:t}^{(l)} \oplus f_t^{(s_1)}$ , where  $\oplus$  refers to concatenate and  $f_{:t}^{(l)}$  means features in timesteps less than  $t$ . We modify the attention mask to ensure that the previous feature seen by  $f_i^{(s_1)}$  is always  $f_{i-1}^{(l)}$ , as shown in the ‘HASS Training Step 2’ part of Figure 3.
- For step  $j \geq 3$ , the feature from the last step  $f_t^{(s_{j-1})}$  is used to calculate the query in timestep  $t + 1$ , while  $f_{:t-j+2}^{(l)} \oplus f_{t-j+2}^{(s_1)} \oplus \dots \oplus f_t^{(s_{j-1})}$  is used to generate keys and values in the self-attention mechanism.

It takes  $n$  times the training overhead of EAGLE and keeps the same decoding overhead. We empirically demonstrate that the acceleration effect is converged with a small  $n$  so that the training of HASS is cost-efficient.

Model	Method	Temperature = 0				Temperature = 1			
		MT-bench	HumanEval	GSM8K	Mean	MT-bench	HumanEval	GSM8K	Mean
L2 7B	PLD	1.43	1.59	1.37	1.46	-	-	-	-
	Lookahead	1.66	1.77	1.65	1.69	-	-	-	-
	EAGLE	3.68	3.90	3.77	3.78	3.45	3.67	3.62	3.58
	EAGLE-2	4.44	4.78	4.60	4.61	4.23	4.47	4.50	4.40
	HASS	<b>4.99</b>	<b>5.29</b>	<b>5.17</b>	<b>5.15</b>	<b>4.84</b>	<b>4.91</b>	<b>5.01</b>	<b>4.92</b>
L2 13B	PLD	1.46	1.70	1.44	1.53	-	-	-	-
	Lookahead	1.64	1.85	1.69	1.73	-	-	-	-
	EAGLE	3.86	4.50	4.17	4.18	3.62	4.27	3.98	3.96
	EAGLE-2	4.74	5.57	5.17	5.16	4.60	5.41	5.03	5.01
	HASS	<b>5.13</b>	<b>6.05</b>	<b>5.55</b>	<b>5.58</b>	<b>4.98</b>	<b>5.86</b>	<b>5.41</b>	<b>5.42</b>
L3 8B	EAGLE	2.91	3.66	3.57	3.38	2.67	3.35	3.30	3.11
	EAGLE-2	4.21	4.93	4.42	4.52	3.90	4.73	4.30	4.31
	HASS	<b>4.68</b>	<b>5.54</b>	<b>5.02</b>	<b>5.08</b>	<b>4.26</b>	<b>5.30</b>	<b>4.85</b>	<b>4.80</b>

Table 1: Acceptance lengths  $\tau$  of different methods on MT-bench, HumanEval, and GSM8K datasets with temperature  $T \in \{0, 1\}$ . L2 represents LLaMA2-Chat, while L3 represents LLaMA3-Instruct.

Model	Method	Temperature = 0				Temperature = 1			
		MT-bench	HumanEval	GSM8K	Mean	MT-bench	HumanEval	GSM8K	Mean
L2 7B	EAGLE	1.90x	2.10x	2.04x	2.01x	1.50x	1.91x	1.87x	1.76x
	EAGLE-2	2.66x	3.06x	2.72x	2.81x	2.39x	2.87x	2.54x	2.60x
	HASS	<b>2.99x</b>	<b>3.41x</b>	<b>3.32x</b>	<b>3.24x</b>	<b>2.70x</b>	<b>3.13x</b>	<b>2.87x</b>	<b>2.90x</b>
L2 13B	EAGLE	1.80x	2.46x	2.41x	2.22x	1.84x	2.10x	2.21x	2.05x
	EAGLE-2	3.02x	3.64x	3.23x	3.30x	3.04x	3.45x	3.13x	3.21x
	HASS	<b>3.23x</b>	<b>4.24x</b>	<b>3.48x</b>	<b>3.65x</b>	<b>3.28x</b>	<b>3.78x</b>	<b>3.37x</b>	<b>3.48x</b>
L3 8B	EAGLE	1.29x	2.00x	1.85x	1.71x	1.25x	1.41x	1.67x	1.44x
	EAGLE-2	2.64x	3.31x	2.54x	2.83x	2.39x	2.54x	2.48x	2.47x
	HASS	<b>2.78x</b>	<b>3.43x</b>	<b>3.06x</b>	<b>3.09x</b>	<b>2.49x</b>	<b>3.05x</b>	<b>2.89x</b>	<b>2.81x</b>

Table 2: Speedup ratios of different methods on MT-bench, HumanEval, and GSM8K datasets with temperature  $T \in \{0, 1\}$ . L2 represents LLaMA2-Chat, while L3 represents LLaMA3-Instruct.

## 4 EXPERIMENT

### 4.1 EXPERIMENTAL SETUP

**Target LLMs.** LLaMA2-Chat 7B/13B and LLaMA3-Instruct 8B.

**Tasks.** We conduct evaluations on three generation tasks. For multi-turn conversation, code generation, and mathematical reasoning tasks, we choose the MT-bench (Zheng et al., 2024), HumanEval (Chen et al., 2021), and GSM8K (Cobbe et al., 2021) datasets, respectively. The batch size is set as 1 under all the experiments following Leviathan et al. (2023) and Zhou et al. (2023).

**Metrics.** HASS neither fine-tunes the target LLMs’ weights during training nor relaxes the acceptance conditions during decoding, making it a lossless acceleration method. Thus, the generation quality is promised with no need for evaluation. We use the following two metrics to assess the acceleration performance:

- **Speedup Ratio:** The actual test speedup ratio w.r.t. vanilla auto-regressive decoding.
- **Acceptance Length  $\tau$ :** The average number of tokens generated per drafting-verification cycle corresponds to the number of tokens accepted by the target model from the draft model.

Note that the speedup ratio is sensitive to the hardware because of the computing power, and the acceptance length is also slightly affected by the hardware because of the numerical error. Therefore, we perform all the inference processes on a single NVIDIA H800 GPU.

**Comparisons.** The vanilla auto-regressive decoding is taken as the baseline, which serves as the benchmark for speedup ratios (1.00x). We compare HASS with recent lossless speculative sampling methods, including PLD (Saxena, 2023), Lookahead (Fu et al., 2023), EAGLE (Li et al., 2024a), and EAGLE-2 (Li et al., 2024b).

**Implementation.** Our code is built based on EAGLE-2’s open source repository<sup>1</sup>. Experiments on EAGLE and EAGLE-2 reuse draft model weights trained by Li et al. (2024a). For harmonized objective distillation,  $K$  is set as 10, and the loss of harmonized objective distillation is added to EAGLE’s original loss with a coefficient of 1.0. For harmonized context alignment, the draft model is aligned for 3 steps during training. For dynamic tree structure, we set the total number of draft tokens to 60 for all experiments with a draft tree depth of 6. We keep other settings, such as the fixed training dataset and the optimizer, consistent with EAGLE-2.

## 4.2 EFFECTIVENESS & ABLATION STUDY

In this section, we first evaluate the effectiveness of HASS by comparing it with existing speculative sampling methods on speedup ratio and acceptance length. Then, we conduct ablation studies on harmonized objective distillation and context alignment.

### 4.2.1 EFFECTIVENESS

We present different methods’ acceptance lengths and speedup ratios across three datasets in Tables 1 and 2, respectively. HASS performs the largest acceptance length and highest speedup ratio across all datasets and LLMs we tested. Most methods achieve their best performance on the HumanEval dataset, as the fixed templates in the code generation task are easier to draft and accelerate. Though PLD and Lookahead are free of training, they consistently show poorer performance than EAGLE, EAGLE-2, and HASS.

### 4.2.2 ABLATION STUDY ON HARMONIZED OBJECTIVE DISTILLATION

We first study the effects of different  $K$  and the weight  $w$  of the Top- $K$  loss by varying these hyper-parameters and summarize the results in Figure 4. Training with the Top- $K$  loss ( $w > 0$ ) always improves performance compared to training without the Top- $K$  loss ( $w = 0$ ). HASS achieves the largest acceptance length when  $w = 0.5$ . A small value of  $K$  ( $K = 1$ ) may result in performance degeneration, as the draft model only focuses on the token with the highest probability and consequently neglects other potential tokens. With a larger  $K$ , the Top- $K$  loss generally brings better results, while the acceptance length is the largest when  $K = 5$ .

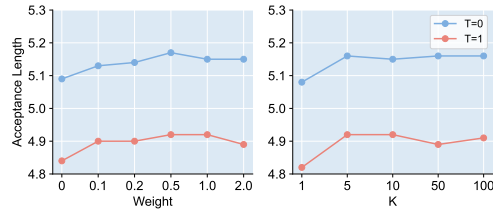


Figure 4: Acceptance lengths  $\tau$  of HASS with varied  $K$ s and weights of the Top- $K$  loss. The results are conducted on LLaMA2-Chat 7B and averaged over MT-bench, HumanEval, and GSM8K datasets with temperature  $T \in \{0, 1\}$ .

We then conduct an experiment with LLaMA2-Chat 7B, where the fixed training dataset is replaced by the dataset generated by the target LLM. We observe that when using non-greedy decoding, the acceptance length increases from 4.92 to 5.19 averaging over three datasets. Therefore, information obtained from harmonized objective distillation is not equivalent to direct distillation from teacher-generated data. A better loss function may exist than Equation 1 to exploit the target LLM further. We leave this topic in future works.

### 4.2.3 ABLATION STUDY ON HARMONIZED CONTEXT ALIGNMENT

We propose the harmonized context alignment, which eliminates the feature inconsistency of draft models between the training and decoding stages. To study the effect of increasing the aligning steps in the harmonized context alignment, we conduct experiments by varying the step number and summarize the results in Table 3.

<sup>1</sup><https://github.com/SafeAILab/EAGLE>

	Aligning Step	MT-bench	HumanEval	GSM8K	Mean
T=0	EAGLE-2 + Top-K	4.59	4.97	4.77	4.78
	HASS Align-2	4.95	5.25	5.12	5.11
	HASS Align-3	<b>4.99</b>	5.29	5.17	5.15
	HASS Align-4	<b>4.99</b>	<b>5.30</b>	<b>5.18</b>	<b>5.16</b>
	HASS Align-5	4.98	5.26	5.09	5.11
T=1	EAGLE-2 + Top-K	4.46	4.61	4.64	4.57
	HASS Align-2	4.71	4.89	4.98	4.86
	HASS Align-3	<b>4.84</b>	4.91	5.01	<b>4.92</b>
	HASS Align-4	4.77	<b>4.93</b>	<b>5.03</b>	4.91
	HASS Align-5	4.71	4.92	4.95	4.86

Table 3: Acceptance lengths  $\tau$  of HASS with varied aligning steps in the harmonized context alignment. The results are conducted on LLaMA2-Chat 7B with temperature  $T \in \{0, 1\}$ .

As the first training step of HASS is the same as EAGLE-2, we continually train EAGLE-2’s draft model weights with the Top-K loss and consider it the baseline. Without harmonized context alignment (EAGLE-2 + Top-K), the draft model performs the worst across all datasets. Training with 3/4 steps of harmonized context alignment generally obtains the most considerable acceptance length. When training with five steps of context alignment, the acceptance length decreases. We believe this is caused by the draft model’s limited capacity, as it predicts less accurately on former steps’ tokens when paying too much attention to the latter ones. Figure 5 shows the acceptance rate  $\alpha$  across speculation steps on MT-bench following Li et al. (2024b). In later speculation steps, HASS performs better acceptance rates than EAGLE-2, demonstrating the effectiveness of harmonized context alignment.

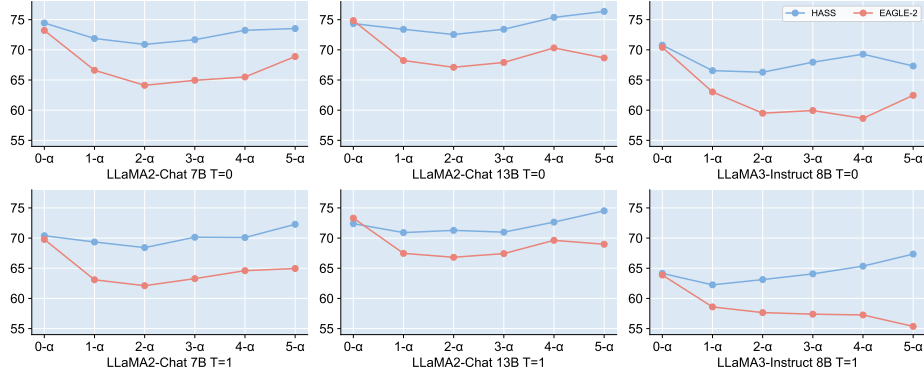


Figure 5: Acceptance rates  $\alpha$  of HASS and EAGLE-2 across different speculation steps on MT-bench with temperature  $T \in \{0, 1\}$ .

## 5 RELATED WORK

There have been a number of works on improving the acceptance rate of speculative sampling while maintaining the target distribution. Most of them fall into two categories. (1) The former category is aligned training that tries to obtain draft models aligned with the target LLM before the decoding stage. Zhou et al. (2023) propose a knowledge distillation approach and studies several strategies to improve the alignment. Li et al. (2024a) demonstrates that hidden states of the target LLM as input of the draft model provide extra feature uncertainty information. Xiao et al. (2024) also utilizes hidden states of the target LLM and introduces an RNN-based draft model design that achieves a comparable acceptance rate. GLIDE (Du et al., 2024) instead reuses kv-cache of the target LLM. It also notices the context misalignment when using information from the target LLM, but the proposed blockwise attention mask method can not solve the misalignment completely. (2) The latter category is efficient decoding, which designs sophisticated decoding strategies to utilize

concurrency efficiently. Miao et al. (2024) proposes to utilize multiple draft models and designs a tree-based attention mechanism to verify multiple draft sequences efficiently. Li et al. (2024b) introduces a dynamic structure to save computation by pruning inefficient paths in the draft tree. Sun et al. (2024) studies improving the verification stage through optimal transportation. However, these works tend to only consider one of training and decoding, ignoring the linkage of these two stages. This work instead aims to link training and decoding, leading to harmonized speculative sampling.

## 6 CONCLUSION

This paper introduces HASS, a harmonized speculative sampling solution that addresses the misalignment between training and decoding on their objectives and contexts. Compared to its closest baseline, EAGLE-2, HASS improves the acceptance rate without any inference overhead. Experiments conducted on LLaMA2-Chat 7/13B, and LLaMA3-Instruct 8B demonstrate the effectiveness and efficiency of HASS. Averaging on MT-bench, HumanEval, and GSM-8K, HASS is 2.81x-3.65x faster than vanilla auto-regressive decoding, 8%-15% faster than EAGLE-2.

## REFERENCES

- Josh Achiam, Steven Adler, Sandhini Agarwal, Lama Ahmad, Ilge Akkaya, Florencia Leoni Aleman, Diogo Almeida, Janko Altschmidt, Sam Altman, Shyamal Anadkat, et al. Gpt-4 technical report. *arXiv preprint arXiv:2303.08774*, 2023.
- Samy Bengio, Oriol Vinyals, Navdeep Jaitly, and Noam Shazeer. Scheduled sampling for sequence prediction with recurrent neural networks. *Advances in neural information processing systems*, 28, 2015.
- Charlie Chen, Sebastian Borgeaud, Geoffrey Irving, Jean-Baptiste Lespiau, Laurent Sifre, and John Jumper. Accelerating large language model decoding with speculative sampling. *arXiv preprint arXiv:2302.01318*, 2023a.
- Mark Chen, Jerry Tworek, Heewoo Jun, Qiming Yuan, Henrique Ponde De Oliveira Pinto, Jared Kaplan, Harri Edwards, Yuri Burda, Nicholas Joseph, Greg Brockman, et al. Evaluating large language models trained on code. *arXiv preprint arXiv:2107.03374*, 2021.
- Ziyi Chen, Xiacong Yang, Jiacheng Lin, Chenkai Sun, Jie Huang, and Kevin Chen-Chuan Chang. Cascade speculative drafting for even faster llm inference. *arXiv preprint arXiv:2312.11462*, 2023b.
- Karl Cobbe, Vineet Kosaraju, Mohammad Bavarian, Mark Chen, Heewoo Jun, Lukasz Kaiser, Matthias Plappert, Jerry Tworek, Jacob Hilton, Reiichiro Nakano, et al. Training verifiers to solve math word problems. *arXiv preprint arXiv:2110.14168*, 2021.
- Cunxiao Du, Jing Jiang, Xu Yuanchen, Jiawei Wu, Sicheng Yu, Yongqi Li, Shenggui Li, Kai Xu, Liqiang Nie, Zhaopeng Tu, et al. Glide with a cape: A low-hassle method to accelerate speculative decoding. *arXiv preprint arXiv:2402.02082*, 2024.
- Angela Fan, Mike Lewis, and Yann Dauphin. Hierarchical neural story generation. *arXiv preprint arXiv:1805.04833*, 2018.
- Yichao Fu, Peter Bailis, Ion Stoica, and Hao Zhang. Breaking the sequential dependency of llm inference using lookahead decoding, November 2023. URL <https://lmsys.org/blog/2023-11-21-lookahead-decoding/>.
- John L Hennessy and David A Patterson. *Computer architecture: a quantitative approach*. Elsevier, 2011.
- Ari Holtzman, Jan Buys, Li Du, Maxwell Forbes, and Yejin Choi. The curious case of neural text degeneration. *arXiv preprint arXiv:1904.09751*, 2019.
- Hsiang-Tsung Kung and John T Robinson. On optimistic methods for concurrency control. *ACM Transactions on Database Systems (TODS)*, 6(2):213–226, 1981.



- Yaniv Leviathan, Matan Kalman, and Yossi Matias. Fast inference from transformers via speculative decoding. In *International Conference on Machine Learning*, pp. 19274–19286. PMLR, 2023.
- Yuhui Li, Fangyun Wei, Chao Zhang, and Hongyang Zhang. Eagle: Speculative sampling requires rethinking feature uncertainty. *arXiv preprint arXiv:2401.15077*, 2024a.
- Yuhui Li, Fangyun Wei, Chao Zhang, and Hongyang Zhang. Eagle-2: Faster inference of language models with dynamic draft trees. *arXiv preprint arXiv:2406.16858*, 2024b.
- Xiaoxuan Liu, Lanxiang Hu, Peter Bailis, Ion Stoica, Zhijie Deng, Alvin Cheung, and Hao Zhang. Online speculative decoding. *arXiv preprint arXiv:2310.07177*, 2023.
- Xupeng Miao, Gabriele Oliaro, Zhihao Zhang, Xinhao Cheng, Zeyu Wang, Zhengxin Zhang, Rae Ying Yee Wong, Alan Zhu, Lijie Yang, Xiaoxiang Shi, et al. Specinfer: Accelerating large language model serving with tree-based speculative inference and verification. In *Proceedings of the 29th ACM International Conference on Architectural Support for Programming Languages and Operating Systems, Volume 3*, pp. 932–949, 2024.
- Apoorv Saxena. Prompt lookup decoding, November 2023. URL <https://github.com/apoorvumang/prompt-lookup-decoding/>.
- Ziteng Sun, Ananda Theertha Suresh, Jae Hun Ro, Ahmad Beirami, Himanshu Jain, and Felix Yu. Spectr: Fast speculative decoding via optimal transport. *Advances in Neural Information Processing Systems*, 36, 2024.
- Jiaxi Tang and Ke Wang. Ranking distillation: Learning compact ranking models with high performance for recommender system. In *Proceedings of the 24th ACM SIGKDD international conference on knowledge discovery & data mining*, pp. 2289–2298, 2018.
- Hugo Touvron, Louis Martin, Kevin Stone, Peter Albert, Amjad Almahairi, Yasmine Babaei, Nikolay Bashlykov, Soumya Batra, Prajjwal Bhargava, Shruti Bhosale, et al. Llama 2: Open foundation and fine-tuned chat models. *arXiv preprint arXiv:2307.09288*, 2023.
- Chaojun Wang and Rico Sennrich. On exposure bias, hallucination and domain shift in neural machine translation. *arXiv preprint arXiv:2005.03642*, 2020.
- Bin Xiao, Lujun Gui, Lei Su, and Weipeng Chen. Clover-2: Accurate inference for regressive lightweight speculative decoding. *arXiv preprint arXiv:2408.00264*, 2024.
- Lianmin Zheng, Wei-Lin Chiang, Ying Sheng, Siyuan Zhuang, Zhanghao Wu, Yonghao Zhuang, Zi Lin, Zhuohan Li, Dacheng Li, Eric Xing, et al. Judging llm-as-a-judge with mt-bench and chatbot arena. *Advances in Neural Information Processing Systems*, 36, 2024.
- Yongchao Zhou, Kaifeng Lyu, Ankit Singh Rawat, Aditya Krishna Menon, Afshin Rostamizadeh, Sanjiv Kumar, Jean-François Kagy, and Rishabh Agarwal. Distillspec: Improving speculative decoding via knowledge distillation. *arXiv preprint arXiv:2310.08461*, 2023.